J. Fluid Mech. (2008), *vol.* 617, *pp.* 283–299.
doi:10.1017/S002211200800431X Printed in the United Kingdom

On the drag-out problem in liquid film theory

E. S. BENILOV† AND V. S. ZUBKOV

Department of Mathematics, University of Limerick, Ireland

(Received 15 February 2008 and in revised form 4 September 2008)

We consider an infinite plate being withdrawn (at an angle α to the horizontal, with a constant velocity U) from an infinite pool of viscous liquid. Assuming that the effects of inertia and surface tension are weak, Derjaguin (*C. R. Dokl. Acad. Sci. URSS*, vol. 39, 1943, p. 13.) conjectured that the 'load' l, i.e. the thickness of the liquid film clinging to the plate, is $l = (\mu U/\rho g \sin\alpha)^{1/2}$, where ρ and μ are the liquid's density and viscosity, and g is the acceleration due to gravity.

In the present work, the above formula is derived from the Stokes equations in the limit of small slopes of the plate (without this assumption, the formula is invalid). It is shown that the problem has infinitely many steady solutions, all of which are stable – but only one of these corresponds to Derjaguin's formula. This particular steady solution can only be singled out by matching it to a self-similar solution describing the non-steady part of the film between the pool and the film's 'tip'.

Even though the near-pool region where the steady state has been established expands with time, the upper, non-steady part of the film (with its thickness decreasing towards the tip) expands faster and, thus, occupies a larger portion of the plate. As a result, the mean thickness of the film is 1.5 times smaller than the load.

1. Introduction

Many industrial coating processes can be modelled by a simple setting where an infinite sloping plate is withdrawn from an infinite pool of viscous liquid (see figure 1*a*). Given that the plate's speed is constant and, eventually, a steady state is established, one usually needs to know the so-called load, i.e. the thickness of the liquid film that the plate carries away from the pool.

This classical problem was originally formulated by Derjaguin in 1943, who conjectured that, if surface tension is negligible and the plate is being withdrawn slowly (hence, the effect of inertia is weak), the load l is

$$l = \left(\frac{\mu U}{\rho g \sin\alpha}\right)^{1/2}, \tag{1.1}$$

where ρ and μ are the liquid density and dynamic viscosity, U is the plate speed, α is the angle between the plate and the horizontal, and g is the acceleration due to gravity. In 1945, Derjaguin supported his conjecture by a quantitative argument; formula (1.1) has also been verified experimentally (Derjaguin & Titievskaya 1945) and numerically (Jin, Acrivos & Münch 2005).

Note, however, that Derjaguin's (1945) argument supporting formula (1.1) was more intuitive than rigorous (see a discussion in Appendix A), and it left several

† Email address for correspondence: eugene.benilov@ul.ie

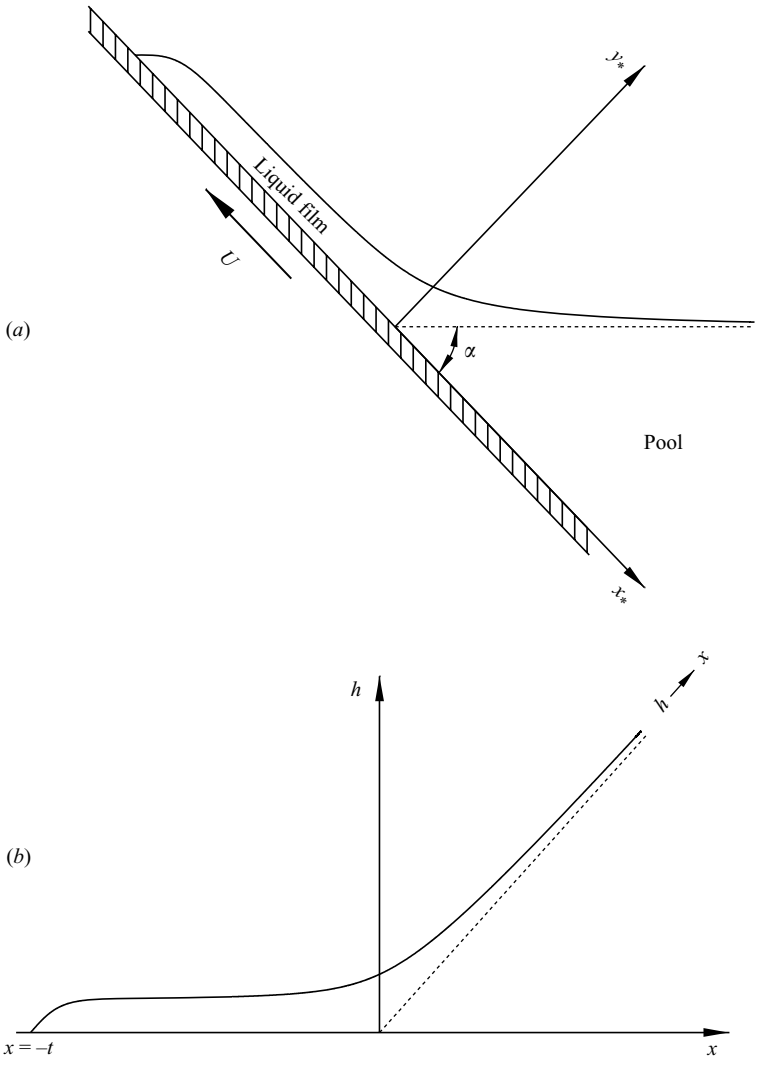

FIGURE 1. Formulation of the problem: (*a*) the setting, (*b*) the mathematical model.

important issues unresolved. First, one can show that the problem admits infinitely many steady solutions, all corresponding to different loads – and it is unclear why the observed value, (1.1), is 'selected' among all the others. Secondly, since formula (1.1) does not have a rigorous mathematical foundation, it is difficult to establish its physical limitations.

In this work, we shall remedy the above shortcomings. We shall demonstrate that the observed steady state (and, hence, the load) is, paradoxically, determined by the *un*steady part of the film adjacent to its 'tip' (no matter how far that has moved away). Furthermore, it will be shown that the film's thickness is close to the load *only near the pool's edge*, while most of the region between the pool and film's tip is unsteady. As a result, the load (being a steady-state characteristic) is not representative of the mean thickness of the film drawn from the pool – but differs from it by an order-one factor. Finally, formula (1.1) will be shown to hold only for moderate values of the plate's slope.

The paper has the following structure: in §2, the problem is formulated mathematically; in §3, we examine the case where the plate's slope is small; and, in §4, the general case is tackled.

2. Formulation of the problem

Let the x_*-axis of the (x_*, y_*) coordinate system (asterisks indicate that the corresponding variables are dimensional) be directed along the plate and downwards – see figure 1(*a*). We shall also introduce the (similarly oriented) velocities (u_*, v_*), the pressure p_*, the film's thickness h_*, and the time t_*.

2.1. *The limit of zero surface tension*

Following Derjaguin (1945), we shall assume that inertia and surface tension are negligible, in which case the flow is governed by the Stokes equations,

$$\frac{\partial p_*}{\partial x_*} = \rho g \sin\alpha + \mu\left(\frac{\partial^2 u_*}{\partial x_*^2} + \frac{\partial^2 u_*}{\partial y_*^2}\right), \quad \frac{\partial p_*}{\partial y_*} = -\rho g \cos\alpha + \mu\left(\frac{\partial^2 v_*}{\partial x_*^2} + \frac{\partial^2 v_*}{\partial y_*^2}\right), \tag{2.1}$$

$$\frac{\partial u_*}{\partial x_*} + \frac{\partial v_*}{\partial y_*} = 0. \tag{2.2}$$

The no-slip and no-flow conditions at the plate are

$$u_* = -U, \qquad v_* = 0 \qquad \text{at} \qquad y_* = 0. \tag{2.3}$$

The kinematic condition at the liquid's surface can be written in a form reflecting mass conservation,

$$\frac{\partial h_*}{\partial t_*} + \frac{\partial}{\partial x_*}\int_0^{h_*} u_* \mathrm{d}y_* = 0, \tag{2.4}$$

whereas the dynamic condition is

$$\boldsymbol{S}_* \boldsymbol{n}_* = \boldsymbol{0} \qquad \text{at} \qquad y_* = h_*, \tag{2.5}$$

where

$$\boldsymbol{S}_* = \begin{bmatrix} 2\mu\dfrac{\partial u_*}{\partial x_*} - p_* & \mu\left(\dfrac{\partial u_*}{\partial y_*} + \dfrac{\partial v_*}{\partial x_*}\right) \\ \mu\left(\dfrac{\partial u_*}{\partial y_*} + \dfrac{\partial v_*}{\partial x_*}\right) & 2\mu\dfrac{\partial v_*}{\partial y_*} - p_* \end{bmatrix}, \qquad \boldsymbol{n}_* = \begin{bmatrix} \dfrac{\partial h_*}{\partial x_*} \\ -1 \end{bmatrix} \tag{2.6}$$

are the stress tensor and a (not necessarily unit) normal to the liquid's surface.

Note that our setting involves a 'contact point', separating the dry and wet parts of the plate – which, generally speaking, requires a certain boundary condition (see Dussan V. 1979; Shikhmurzaev 2006, and references therein). As a result, a boundary layer occurs near the contact point. The width of this layer, however, is extremely small, and all of the previous researchers dealing with the drag-out problem neglected its effect.

Accordingly, we shall assume that the effect of 'dewetting' is negligible and the contact point moves together with the plate–which corresponds to the following boundary condition:

$$h_* = 0 \qquad \text{at} \qquad x_* = -Ut_*. \tag{2.7}$$

At large distances from the edge of the pool, the pool's surface is unperturbed, i.e.

$$h_* \to (\tan\alpha)x_* \qquad \text{as} \qquad x_* \to +\infty. \tag{2.8}$$

The boundary-value problem (2.1)–(2.8) determines the flow in the domain

$$-Ut_* < x_* < +\infty, \qquad 0 < y_* < h_*.$$

Next we introduce the following non-dimensional variables:

$$x = \frac{\varepsilon x_*}{l}, \qquad y = \frac{y_*}{l}, \qquad t = \frac{\varepsilon U t_*}{l}, \qquad h = \frac{h_*}{l}, \tag{2.9}$$

$$u = \frac{u_*}{U}, \qquad v = \frac{v_*}{\varepsilon U}, \qquad p = \frac{(1+\varepsilon^2)^{1/2} p_*}{\rho g l}, \tag{2.10}$$

where l is defined by (1.1) and

$$\varepsilon = \tan\alpha$$

(the use of symbol ε does not necessarily imply that $\tan\alpha \ll 1$). Substituting (2.9)–(2.10) into the Stokes set (2.1)–(2.8), we obtain

$$\frac{\partial p}{\partial x} = 1 + \varepsilon^2 \frac{\partial^2 u}{\partial x^2} + \frac{\partial^2 u}{\partial y^2}, \qquad \frac{\partial p}{\partial y} = -1 + \varepsilon^4 \frac{\partial^2 v}{\partial x^2} + \varepsilon^2 \frac{\partial^2 v}{\partial y^2}, \tag{2.11}$$

$$\frac{\partial u}{\partial x} + \frac{\partial v}{\partial y} = 0, \tag{2.12}$$

$$u = -1, \qquad v = 0 \qquad \text{at} \qquad y = 0, \tag{2.13}$$

$$\left(2\varepsilon^2 \frac{\partial u}{\partial x} - p\right)\frac{\partial h}{\partial x} - \left(\frac{\partial u}{\partial y} + \varepsilon^2 \frac{\partial v}{\partial x}\right) = 0 \qquad \text{at} \qquad y = h, \tag{2.14}$$

$$\varepsilon^2 \left(\frac{\partial u}{\partial y} + \varepsilon^2 \frac{\partial v}{\partial x}\right)\frac{\partial h}{\partial x} - \left(2\varepsilon^2 \frac{\partial v}{\partial y} - p\right) = 0 \qquad \text{at} \qquad y = h, \tag{2.15}$$

$$\frac{\partial h}{\partial t} + \frac{\partial}{\partial x}\int_0^h u \, \mathrm{d}y = 0, \tag{2.16}$$

$$h = 0 \qquad \text{at} \qquad x = -t, \tag{2.17}$$

$$h \to x \qquad \text{as} \qquad x \to +\infty. \tag{2.18}$$

In what follows, equations (2.11)–(2.18) will be used when the plate's slope is order-one. If, however, it is small,

$$\varepsilon \ll 1,$$

one can take advantage of the lubrication approximation.

Following the usual routine of lubrication analysis, one can treat (2.11)–(2.15) as a boundary-value problem for u, v, and p and express them as expansions in ε^2, e.g.

$$u = -1 + \left(hy - \frac{y^2}{2}\right)\left(1 - \frac{\partial h}{\partial x}\right) + O(\varepsilon^2). \tag{2.19}$$

Substituting this equality into (2.16) and omitting the $O(\varepsilon^2)$ terms, we obtain

$$\frac{\partial h}{\partial t} + \frac{\partial}{\partial x}\left(-h + \frac{h^3}{3} - \frac{h^3}{3}\frac{\partial h}{\partial x}\right) = 0. \tag{2.20}$$

Note that the first term in the brackets corresponds to entrainment of the liquid by the plate's motion, the second term describes the effect of gravity, and the last one the hydrostatic pressure gradient due to variations of the film's thickness. Similar equations have been derived, for similar problems, by Moriarty, Schwartz & Tuck (1991), Bertozzi & Brenner (1997), and Kalliadasis, Bielarz & Homsy (2000).

Finally, the asymptotic equivalents of the boundary conditions (2.17)–(2.18) are

$$h = 0 \qquad \text{at} \qquad x = -t, \tag{2.21}$$

$$h \to x \qquad \text{as} \qquad x \to +\infty. \tag{2.22}$$

The boundary-value problem (2.20)–(2.22) is illustrated in figure 1(*b*).

2.2. *The effect of surface tension*

As mentioned before, this paper is concerned with the limit of negligible surface tension, but it is still instructive to briefly discuss the capillary-modified version of equation (2.20). Its derivation is very similar to that of (2.20), resulting in

$$\frac{\partial h}{\partial t} + \frac{\partial}{\partial x}\left(-h + \frac{h^3}{3} - \frac{h^3}{3}\frac{\partial h}{\partial x} + \frac{\gamma h^3}{3}\frac{\partial^3 h}{\partial x^3}\right) = 0,$$

where

$$\gamma = \frac{\sigma(\tan\alpha)^3}{\mu U} \tag{2.23}$$

is the non-dimensional parameter characterizing the importance of capillary effects (σ is the surface tension, recall also that μ is the viscosity and U, the plate's velocity).

To illustrate expression (2.23), let the liquid under consideration be glycerine at 20 °C, for which

$$\mu \approx 1.41 \text{kg m}^{-1}\,\text{s}^{-1}, \qquad \sigma \approx 0.063\,\text{N m}^{-1}.$$

Then, for a moderately small angle $\alpha = \frac{1}{9}\pi$, and a velocity $U = 0.1\text{m s}^{-1}$, formula (2.23) yields $\gamma \approx 0.043$ – which can be safely regarded as a small parameter. Furthermore, with the exception of mercury, surface tensions of common liquids range within $0.02 - 0.08\,\text{N m}^{-1}$, whereas the corresponding viscosities may differ by up to two orders of magnitude. The viscosity of industrial polymers, for example, often reaches $40\,\text{kg s}^{-1}\text{m}^{-1}$, while that of liquid foods – such as ketchup, mustard, or peanut butter – ranges from 50 to $250\,\text{kg s}^{-1}\text{m}^{-1}$.

Thus, in many applications, γ is very small and capillary effects are negligible.

3. The small-slope limit

It appears obvious (and will be verified later) that, even though a steady state emerges near the edge of the pool, the film's 'tip' always remains non-steady. At large times ($t \gg 1$), the two regions become well separated and can be examined separately – see § 3.1. Then, in § 3.2, the asymptotic results will be verified and complemented by direct simulation of the small-slope equation (2.20).

3.1. *Asymptotic results for* $t \gg 1$

For a steady solution, $h = \bar{h}(x)$, equation (2.20) yields

$$-\bar{h} + \frac{\bar{h}^3}{3} - \frac{\bar{h}^3}{3}\frac{\mathrm{d}\bar{h}}{\mathrm{d}x} = q \tag{3.1}$$

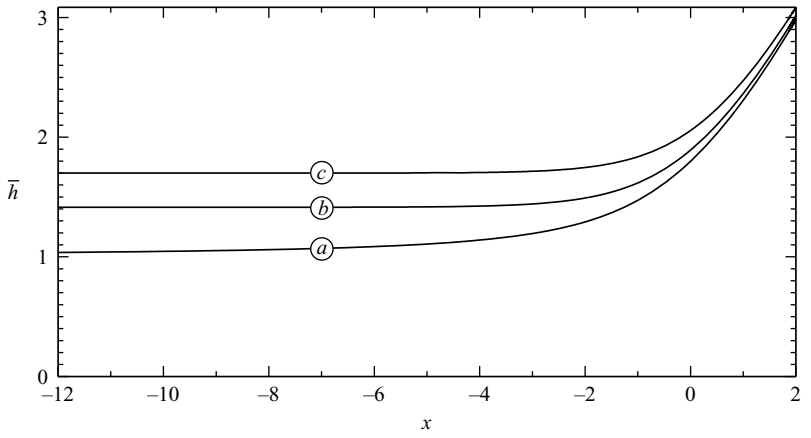

FIGURE 2. The film's thickness $\bar{h}(x)$ of a steady drag-out flow (determined by the boundary-value problem (3.1)–(3.4)), for various values of the non-dimensional load: (*a*) $\bar{h}_0 = 1$, (*b*) $\bar{h}_0 = \sqrt{2}$, (*c*) $\bar{h}_0 = 1.7$. Solutions (*a*) and (*b*) correspond to the endpoints of range (3.5).

where the constant of integration q is, physically, the non-dimensional flux of liquid carried by the plate. We shall also require

$$\bar{h} \to \bar{h}_0 \qquad \text{as} \qquad x \to -\infty, \tag{3.2}$$

where $\bar{h}_0$ is the non-dimensional load, i.e. the thickness of the film carried by the plate infinitely far from the pool. Taking the limit $x \to -\infty$ in (3.1) and taking into account (3.2), we obtain

$$q = -\bar{h}_0 + \tfrac{1}{3}\bar{h}_0^3. \tag{3.3}$$

Finally, condition (2.22) (which matches the film to the pool) yields

$$\bar{h} \to x \qquad \text{as} \qquad x \to +\infty. \tag{3.4}$$

Equation (3.1) is separable and, thus, boundary-value problem (3.1)–(3.4) can be readily solved (the actual solution is not presented here, as it is bulky – but several examples are shown in figure 2). Most importantly, solutions exist for *all* $\bar{h}_0 \geqslant 1$, i.e. the steady-state problem leaves the load undetermined.

The allowable range of $\bar{h}_0$, however, can be reduced by analysing expression (2.19) for the liquid's velocity. Estimating its sign at $y = h$, one can see that, for $h > \sqrt{2}$, the film's top layers slide back towards the pool – which corresponds to a source of liquid located at minus-infinity and makes the solution irrelevant physically. Still, all values in the range

$$1 \leqslant \bar{h}_0 \leqslant \sqrt{2} \tag{3.5}$$

appear to give rise to physically meaningful steady solutions. Only one of these, however, corresponds to the 'correct' (experimentally verified) formula (1.1) for the dimensional load.

We note that paradoxes resulting from multiple solutions can often be resolved by a stability analysis (which would usually show that all solutions, except one, are unstable). In the present case, however, *all* solutions corresponding to range (3.5) are stable (see Appendix B).

As it turns out, the 'correct' value of the load $\bar{h}_0$ can only be identified by studying the non-steady part of the film. Fortunately, that happens to be described by a

relatively simple self-similar solution–which, however, does not necessarily match the steady solution near the pool. The only value of $\bar{h}_0$ for which the two solutions do match is the 'correct' one.

To find the solution describing the non-steady part of the film, let

$$h(x, t) = t^{-1} f(\xi), \tag{3.6}$$

where

$$\xi = (x + t)t \tag{3.7}$$

(this substitution corresponds to a self-similar behaviour in the reference frame associated with the film's tip). Substitution of (3.6)–(3.7) into equation (2.20) yields

$$-f + f'\xi - \left[\frac{f^3}{3}(f' - 1)\right]' = 0. \tag{3.8}$$

The condition at the tip of the film, (2.21), implies

$$f(0) = 0.$$

We have found three distinct asymptotics of equation (3.8) compatible with the above boundary condition (and are reasonably sure that none has been missed):

$$f \to a\xi^{1/4} + \tfrac{4}{7}\xi + O\left(\xi^{5/4}\right) \qquad \text{as} \qquad \xi \to +0 \tag{3.9}$$

or

$$f = \xi + a\exp[-3\xi^{-1} - 2\ln\xi + O(\xi)] \qquad \text{as} \qquad \xi \to +0 \tag{3.10}$$

(in both cases, a is arbitrary) or

$$f = a\xi + a^3(a - 1)\xi^2 + O(\xi^3) \qquad \text{as} \qquad \xi \to +0 \tag{3.11}$$

($a \neq 1$).

To distinguish between the three possible asymptotics, note that the evolutionary equation (2.20) preserves the slope at the film's tip (see Appendix C). Then, assuming that our solution originates from the initial condition where the pool's surface is unperturbed (hence, $\partial h/\partial x = 1$), we conclude that the desired asymptotic is (3.10). Asymptotics (3.9) implies an infinite slope at $\xi = 0$, whereas (3.11) implies a finite one, but it still does not match the derivative of the initial condition.

At large ξ, in turn, equation (3.8) yields

$$f = \xi^{1/2} + \tfrac{1}{12}\ln\xi + b + O\left(\xi^{-1/2}\ln^2\xi\right) \qquad \text{as} \qquad \xi \to +\infty \tag{3.12}$$

or

$$f = \xi + b(1 + 3\xi^{-1} + 9\xi^{-2}\ln\xi) + c\xi^{-2} + O(\xi^{-3}\ln\xi) \qquad \text{as} \qquad \xi \to +\infty,$$

where b and c are arbitrary. It can be verified, however, that the latter asymptotic cannot be matched to the steady solution $\bar{h}(x)$ near the pool and, thus, is irrelevant to the problem at hand.

To match the remaining asymptotic, (3.12), to $\bar{h}(x)$, assume that x is far from the pool, but not too close to the film's tip,

$$1 \ll -x \ll t \tag{3.13}$$

(which, obviously, implies that $t \gg 1$). Then, in solution (3.6)–(3.7), we can replace f with asymptotics (3.12) and obtain

$$h \approx t^{-1}\sqrt{(x + t)t} \approx 1. \tag{3.14}$$

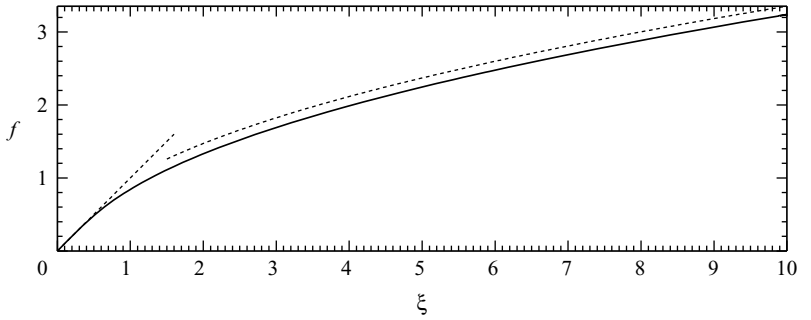

FIGURE 3. The shape of the self-similar part of the film (i.e. the numerical solution of the boundary-value problem (3.8), (3.10), (3.12)). The dotted lines correspond to the asymptotics given by the first term of (3.10) and the first two terms of (3.12).

Next, recall that, in region (3.13), the steady solution $\bar{h}(x)$ is close to its limiting value $\bar{h}_0$ – hence, it can be matched to the limiting value (3.14) of the self-similar solution only if

$$\bar{h}_0 = 1. \tag{3.15}$$

Recalling how h (and, hence, $\bar{h}_0$) were non-dimensionalized (see (2.9)–(2.10)), one can see that (3.15) agrees with formula (1.1) for the dimensional load l.

To complete our asymptotic results, we present the (implicit) solution of the steady problem (3.1)–(3.4) corresponding to the 'correct' value $\bar{h}_0 = 1$,

$$9\bar{h} + 8\ln\left(\frac{\bar{h}-1}{\bar{h}+2}\right) - \frac{3}{\bar{h}-1} = 9x. \tag{3.16}$$

We shall also need the function $f(\xi)$ which describes the shape of the non-steady part of the film. To find it, we solved the boundary-value problem (3.8), (3.10), (3.12) numerically. Instead of zero and plus-infinity, the boundary conditions were set at a small and large values of ξ, with the corresponding values of f determined by the first term of asymptotic (3.10) and the first two terms of asymptotic (3.12), respectively. The resulting problem was solved through an iterative procedure based on Newton's method, and the solution is shown in figure 3.

Summarizing this subsection, we present the composite asymptotic solution,

$$h(x,t) \approx \bar{h}(x) + t^{-1} f[(x+t)t] - 1, \tag{3.17}$$

where $\bar{h}(x)$ is the steady solution emerging near the pool (given by (3.16)); $f(\xi)$ describes the shape of the film's non-steady upper part (determined by (3.8), (3.10), (3.12)); and the unity represents the common part of the two solutions. In the limit $t \to \infty$, (3.17) holds for *all* values of x.

3.2. *Simulation of the evolutionary equation (2.20)*

Since our asymptotic solution (3.17) is applicable only for large t, it cannot be traced back to $t = 0$. As a result, we cannot verify that it corresponds to the initial condition that we are interested in–the one corresponding to the pool's surface being unperturbed, i.e.

$$h = x \qquad \text{at} \qquad t = 0. \tag{3.18}$$

This issue can only be resolved by direct simulation of the small-slope equation (2.20).

The initial/boundary-value problem (2.20)–(2.22), (3.18) was integrated using the finite-element solver available in the COMSOL Multiphysics package. The solution

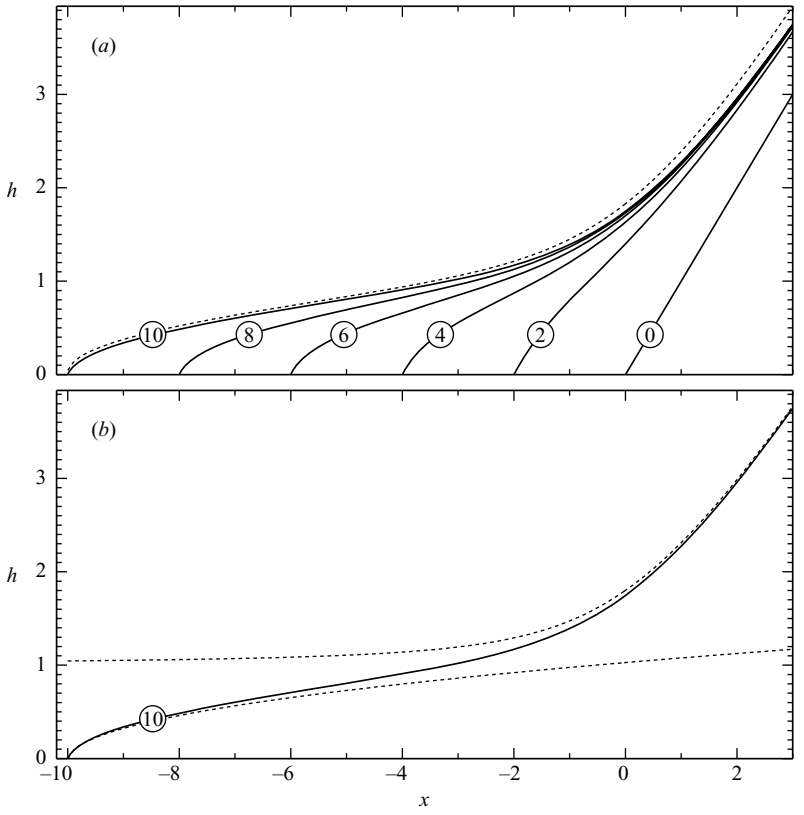

FIGURE 4. The evolution of the film for the small-slope case (determined by the initial/boundary-value problem (2.20)–(2.22), (3.18)). The curves are labelled with the corresponding values of the time t. The solid curves show the numerical solution, the dotted curves show: (a) the composite asymptotic solution (3.17), (b) the steady solution (3.16) and the self-similar solution (3.6)–(3.7).

computed, as well as the composite asymptotic solution (3.17), are shown in figures 4 and 5.

One can see that, at $t = 10$, the two solutions agree reasonably well; at $t = 20$, they are difficult to distinguish; and, for $t \geqslant 30$, virtually indistinguishable. In addition to the composite asymptotic solution, we show its 'components' (the steady and self-similar solutions) in figure 4(b).

Observe that, even for the long-term evolution shown in figure 6(a), there seems to be no visible sectoin where the solution is horizontal, i.e. equal to the load. Moreover, the emerging steady state becomes 'visible' only if a small area near the pool's edge is enlarged (as in figure 6(b)). The reason for this is that the steady-state region (with h approximately equal to the load) expands much slower than the non-steady region (with variable h)–hence, the portion of the plate occupied by the former is much smaller than that occupied by the latter.

This circumstance has crucial implications for the mean thickness of the film (which is the most important characteristic of the drag-out process). If the solution outside the pool were steady, the mean thickness would be equal to the load l, but, since the film is mainly unsteady and its thickness varies from l to 0, the mean is less than l.

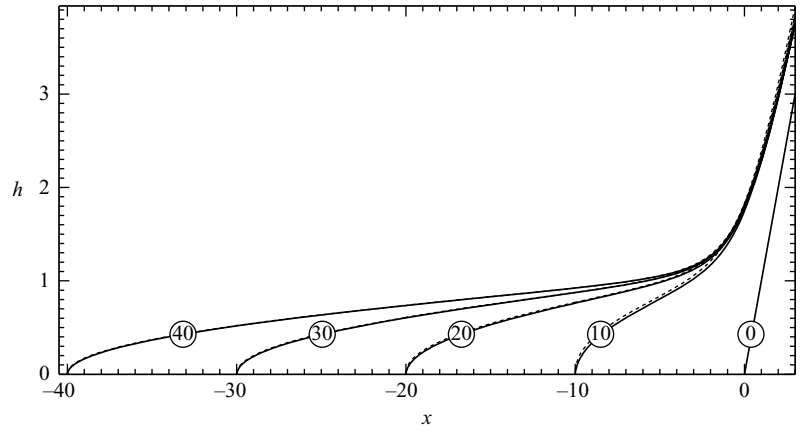

FIGURE 5. The evolution of the film for the small-slope case (determined by (2.20)–(2.22), (3.18)). The curves are labelled with the corresponding values of the time t. The solid curves show the numerical solution, the dotted curves show the composite asymptotic solution (3.17) (for $t \geqslant 30$, the numerical and asymptotic curves are virtually indistinguishable).

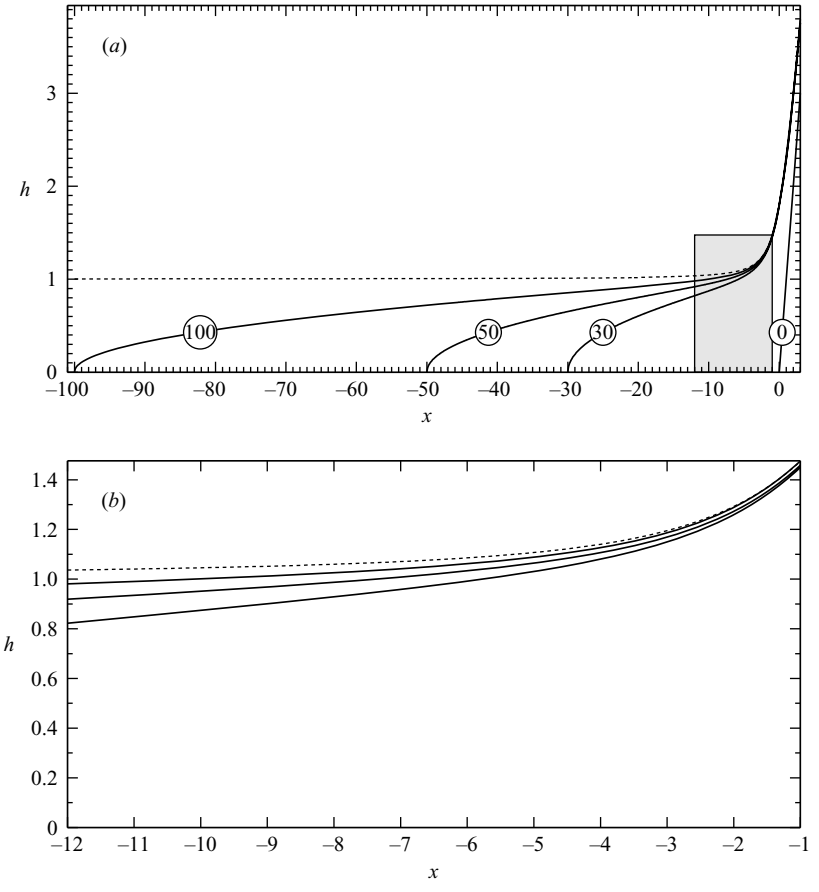

FIGURE 6. The evolution of the film for the small-slope case (determined by (2.20)–(2.22), (3.18)). The curves are labelled with the corresponding values of the time t. The solid curves show the numerical solution, the dotted curve shows the steady solution (3.16). The area shaded in panel (a) corresponds (b) (the latter illustrating the emergence of the steady state near the edge of the pool).

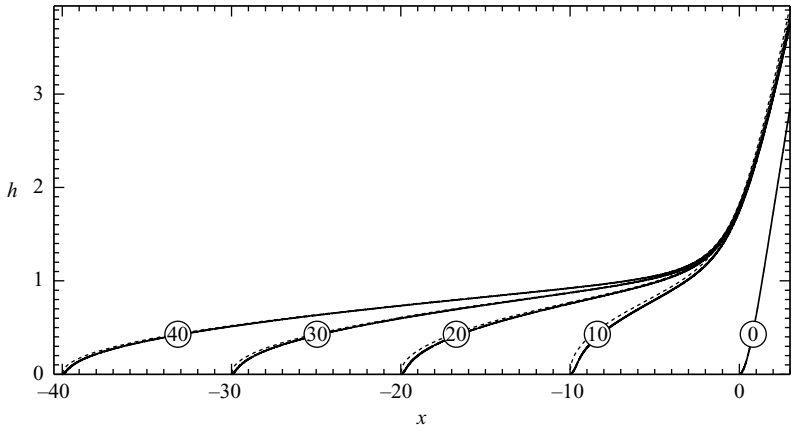

FIGURE 7. The same as in figure 5, but for the initial condition (3.19)–(3.20) instead of (3.18).

To calculate the mean thickness for $t \gg 1$, one can approximate the profile of the self-similar solution, $f(\xi)$, by its large-distance asymptotics (3.12) (which is not valid only in a relatively small region adjacent to the film's tip). Thus, taking into account that the length of the film grows linearly with time, we obtain

$$\text{mean non-dimensional thickness} = \lim_{t\to\infty} \frac{1}{t} \int_{-t}^{0} t^{-1} \sqrt{(x+t)\,t}\, \mathrm{d}x = \tfrac{2}{3}.$$

Dimensionally, this implies that the film's mean thickness is 1.5 times smaller than the load given by formula (1.1).

Finally, we shall discuss what happens if the pool's surface is initially perturbed. In particular, let the initial condition have non-unit derivative at the pools's boundary, i.e.

$$\left(\frac{\partial h}{\partial x}\right)_{x=0} \neq 1 \qquad \text{at} \qquad t = 0.$$

Then, since the slope at the film's tip is conserved (see Appendix C), such initial conditions seem to be incompatible with our self-similar solution (3.6)–(3.7), (3.10) for which $\partial h/\partial x$ at the film's tip equals unity.

The simplest option in this case appears to be replacing the boundary condition (3.10) with (3.11) which allows non-unit derivative at $\xi = 0$, i.e. at the film's tip. It turns out, however, that the resulting boundary-value problem, (3.8), (3.11)–(3.12), has no solution. (This is not a mathematical theorem but rather a conclusion based on numerical evidence.)

To resolve this issue, the small-slope equation (2.20) was simulated for various initial conditions with non-unit derivative at the film's tip. Typical results, computed for

$$h = x + kxe^{-x} \qquad \text{at} \qquad t = 0, \tag{3.19}$$

with

$$k = -1, \tag{3.20}$$

are shown in figure 7. One can see that the asymptotic solution (3.17) agrees with the numerical one everywhere except the vicinity of the film's tip. Most importantly, the 'disagreement region' rapidly contracts with time and has no influence whatsoever on the load or other global characteristics.

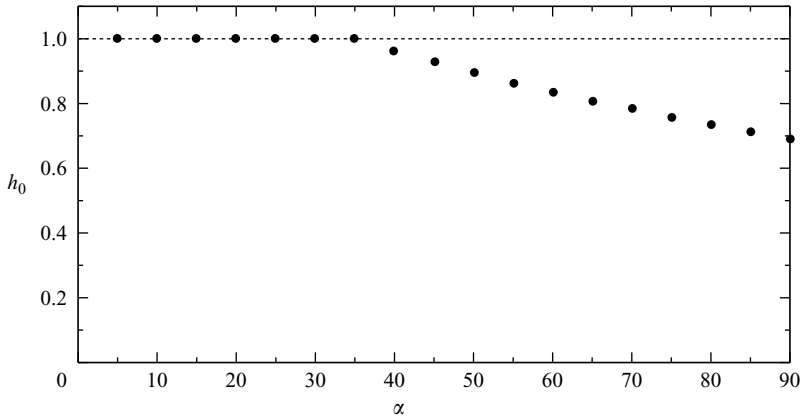

FIGURE 8. The non-dimensional load (as determined by the Stokes equations (2.11)–(2.18)) *vs.* the angle α of the plate's slope. The dotted line corresponds to the small-α asymptotic result, (3.15).

The same pattern was observed for other values of k, as well as other initial conditions.

4. The case of finite slope

If the slope of the film's surface is not small, the Stokes equations (2.11)–(2.18) do not involve small parameters and can only be solved numerically. This task has been carried out originally by Jin *et al.* (2005) for a more general model including surface tension. In the present work, in turn, surface tension is neglected, as we need to verify our asymptotic results presented above.

The Stokes equations (2.11)–(2.18) were integrated using the Moving Mesh (ALE) and Incompressible Navier–Stokes modules of the COMSOL Multiphysics. The parameters were chosen in such a way that, in all runs, the Reynolds number was 10^{-4}, so inertia was negligible. Starting from an appropriate initial condition, the problem was simulated until a steady state had been established everywhere in the computational region, after which the load could be measured. The results are shown in figure 8.

One can see that the small-slope approximation works for fairly large angles, $\alpha \lesssim 35^\circ$. Furthermore, its error in this range is 10^{-3}, which is a great deal better than expected. Indeed, the small-slope equation (2.20) was derived by omitting $O[(\tan\alpha)^2]$ and smaller terms from the Stokes set–hence, for $\alpha \approx 35^\circ$, the truncation error should be about $(\tan 35^\circ)^2 \approx 0.53$. This discrepancy suggests that some (probably more than one) of the next-order corrections to the asymptotic load $\bar{h}_0$ cancel out, improving the effective accuracy of the leading-order formula.

Observe also the abrupt turn with which the numerical curve splits from its asymptotic counterpart at $\alpha \approx 35^\circ$. It appears that a pitchfork bifurcation occurs at this point: the 'old' solution loses stability and the system switches to a lower branch. Such an explanation implies that there exists another stable solution, corresponding to the upper branch (i.e. with a load higher than the observed one) – however, it has never appeared in our simulations.

To resolve the discrepancy, recall that the evolution begins from the initial condition with a zero load; as a result, the system cannot reach the high-load solution without

passing through the low-load one. The latter, however, is a steady state, and, once it is reached, the system stops evolving and remains there indefinitely.

In other words, the high-load solution, if it exists, cannot be computed if the liquid is initially at rest and the pool's surface is unperturbed – nor can it be observed (for the same reason) in the 'real' world.

5. Summary and concluding remarks

We have examined the flow of a viscous liquid induced by an infinite sloping plate being withdrawn from an infinite pool. It was conjectured (Derjaguin 1943) that the load l, i.e. the thickness of the liquid film clinging to the plate, is given by formula (1.1). This conjecture, however, was not supported by a consistent calculation, and none has followed since 1943.

In the present paper, formula (1.1) for l is derived from the Stokes set under an additional assumption that the plate's slope is small, in which case a relatively simple asymptotic equation, (2.20), can be derived. It is shown that (2.20) has infinitely many steady solutions, all of which are stable, but only one of these corresponds to formula (1.1). This particular steady solution, (3.16), is then identified by matching it to a self-similar solution for the film's non-steady upper part (described by (3.6)–(3.7), (3.8), (3.10), (3.12)). The two asymptotic solutions are eventually combined as a composite solution, (3.17), which is applicable everywhere. It is demonstrated (by direct simulation of equation (2.20), see § 3.2) that the composite solution is an attractor and, thus, provides large-time asymptotics for a wide class of initial conditions.

It is also shown that, even though the region where the steady state has been established expands with time, the upper part of the film (with its thickness decreasing towards the tip) expands faster. As a result, the mean value of the film's thickness is 1.5 times smaller than the load.

We have also carried out direct simulations of the Stokes set and, thus, showed that the small-slope approximation is valid when the angle of the plate's slope is less than, approximately, 35°. Remarkably, its accuracy within this range is about 10^{-3}, which is exceptionally high.

Finally, it would be interesting to extend the present approach to capillary effects and compare the results with the extensive body of literature on steady drag-out flows with surface tension (Landau & Levich 1942; Wilson 1982, etc.).

This work was supported by the Science Foundation Ireland through the Mathematics Applications Consortium for Science and Industry (MACSI).

Appendix A. The paper by Derjaguin (1945)

Unlike our work, Derjaguin (1945) (whose paper will be referred to as D45) assumes the plate to be motionless and the level of liquid in the pool to be dropping at a constant speed. This setting can be obtained from ours by changing the latter to the reference frame co-moving with the plate.

The two approaches differ also in a more substantial way: unlike our work, D45 neglects the pressure gradient associated with variations of the film's thickness. In terms of our non-dimensional variables, this amounts to

$$\left|\frac{\partial h}{\partial x}\right| \ll 1. \tag{A 1}$$

Accordingly, the last term in the small-slope equation (2.20) can be omitted, which yields

$$\frac{\partial h}{\partial t} + \frac{\partial}{\partial x}\left(-h + \frac{h^3}{3} \right) = 0 \tag{A 2}$$

(observe that the change of variables $x_{co-moving} = x + t$ transforms (A 2) into D45's equation (8)). The general solution of (A 2) can be readily found (in an implicit form) by the method of characteristics,

$$x = F(h) + (-1 + h^2)t. \tag{A 3}$$

The function $F(h)$ is determined by the initial condition, which, somewhat unexpectedly, D45 assumes to be

$$h = \infty \qquad \text{for} \qquad t = 0, \qquad x > 0 \tag{A 4}$$

(see D45's equation (10)). Eventually, D45 concludes that $F(h) = 0$ and (A 3) yields

$$h = \sqrt{\frac{x}{t} + 1}. \tag{A 5}$$

Note that D45's condition (A 4) implies that the angle between the plate and the pool's surface is 90°, whereas a more sensible assumption would be that it is α. In terms of our non-dimensional variables (see (2.9)–(2.10)), the latter amounts to

$$h = x \qquad \text{for} \qquad t = 0, \qquad x > 0.$$

Accordingly, the undetermined function in (A 3) becomes $F(h) = h$, and (A 3) yields

$$h = \sqrt{\frac{x}{t} + 1 + \frac{1}{4t^2}} - \frac{1}{2t}. \tag{A 6}$$

This solution rectifies the inconsistency resulting from the incorrect initial condition (A 4). Note also that, as $t \to \infty$, the correct and incorrect solutions, (A 6) and (A 5), 'forget' their respective initial conditions and merge.

Unfortunately, D45 contains another inconsistency, one that cannot be easily rectified. It has several manifestations: first, it follows from (A 6) that

$$h \to \sqrt{\frac{x}{t}} \qquad \text{as} \qquad x \to +\infty,$$

which is inconsistent with the boundary condition (2.22) and, thus, does not match the pool. Secondly, even if it did (i.e. if $h \approx x$ for large x), it would imply $\partial h/\partial x \approx 1$, which violates assumption (A 1) on which the original equation (A 2) is based. Thirdly, assumption (A 1) is also violated near the film's tip ($x \sim -t$) and the liquid level ($x \sim 0$).

In other words, D45 should have used the 'full' equation (2.20) instead of the truncated one, (A 2). (Note that (A 2) is still valid where the film's slope is small, e.g. far from both the film's tip and the pool (provided these regions are far apart, i.e. for large t). In this case, the corresponding limit of solution (A 6) coincides with the 'correct' solution (3.6)–(3.7) where $f(\xi)$ is replaced with its large-ξ asymptotics, i.e. the first term of (3.12).).

Appendix B. Stability of steady solutions of equation (2.20)

Let

$$h = \bar{h}(x) + \tilde{h}(x, t), \tag{B 1}$$

where $\bar{h}$ is a steady solution of the small-slope equation (2.20) and $\tilde{h}$ is a disturbance. Substituting (B 1) into (2.20) and linearizing, we obtain

$$\frac{\partial \tilde{h}}{\partial t} + \frac{\partial}{\partial x}\left(-\tilde{h} + \bar{h}^2\tilde{h} - \bar{h}^2\tilde{h}\frac{\mathrm{d}\bar{h}}{\mathrm{d}x} - \frac{\bar{h}^3}{3}\frac{\partial \tilde{h}}{\partial x}\right) = 0. \tag{B 2}$$

We shall confine ourselves to solutions with exponential dependence on t,

$$\tilde{h}(x, t) = \phi(x)\, e^{\lambda t},$$

for which (B 2) yields

$$\lambda\phi + \frac{\mathrm{d}}{\mathrm{d}x}\left(-\phi + \bar{h}^2\phi - \bar{h}^2\phi\frac{\mathrm{d}\bar{h}}{\mathrm{d}x} - \frac{\bar{h}^3}{3}\frac{\mathrm{d}\phi}{\mathrm{d}x}\right) = 0. \tag{B 3}$$

We shall assume that the disturbance is bounded at infinity, i.e.

$$|\phi| < \infty \qquad \text{as} \qquad x \to \pm\infty. \tag{B 4}$$

(B 3)–(B 4) form an eigenvalue problem, where ϕ is the eigenfunction and λ is the eigenvalue. If there exists an eigenvalue such that $\mathrm{Re}\lambda > 0$, the steady state $\bar{h}(x)$ is unstable.

Observe that, since $\bar{h} \to \bar{h}_0$ as $x \to -\infty$, (B 3) yields

$$\phi \to C_1 \exp\left(\sqrt{\frac{3\lambda}{\bar{h}_0^3}}x\right) + C_2 \exp\left(-\sqrt{\frac{3\lambda}{\bar{h}_0^3}}x\right) \qquad \text{as} \qquad x \to -\infty, \tag{B 5}$$

where $C_{1,2}$ are constants of integration. Then, it follows that ϕ does not tend to zero (but oscillates) only if

$$\mathrm{Re}\lambda < 0, \qquad \mathrm{Im}\lambda = 0;$$

such solutions are stable and, thus, do not need further examination. In all other cases, condition (B 4) requires one of the constants $C_{1,2}$ be zero, and (B 5) results in

$$\phi \to 0 \qquad \text{as} \qquad x \to -\infty. \tag{B 6}$$

To analyse the behaviour of ϕ as $x \to +\infty$, we shall need the corresponding asymptotics of $\bar{h}(x)$ (which can be extracted from (3.1)–(3.4)):

$$\bar{h} = x + 3x^{-1} + O(x^{-2}) \qquad \text{as} \qquad x \to +\infty.$$

Then, as follows from (B 3),

$$\phi = C_1[1 + O(x^{-1})] + C_2[x^{-2} + O(x^{-3})] \qquad \text{as} \qquad x \to +\infty.$$

Note that solutions with $C_1 \neq 0$ involve changes of the liquid's level in the pool far away from its edge and, thus, are irrelevant to the stability of the drag-out flow (moreover, it can be shown that they imply $\lambda = 0$, i.e. are stable anyway). As a result, we can assume

$$\phi \to 0 \qquad \text{as} \qquad x \to +\infty. \tag{B 7}$$

In what follows, it is convenient to move the boundary conditions (B 6)–(B 7) from infinity to finite points,

$$\phi = 0 \qquad \text{at} \qquad x = x_{\pm}, \tag{B 8}$$

then take the limit $x_- \to -\infty$, $x_+ \to +\infty$ (the advantages of this approach will be explained later).

Next, we introduce a new variable ψ such that

$$\phi = \frac{\psi}{\bar{h}^3} \exp\left(3 \int \frac{\bar{h}^2 - 1}{\bar{h}^3} \, \mathrm{d}x\right).$$

In terms of ψ, the eigenvalue problem (B 3), (B 8) is

$$\lambda \frac{\psi}{\bar{h}^3} \exp\left(3 \int \frac{\bar{h}^2 - 1}{\bar{h}^3} \mathrm{d}x\right) = \tfrac{1}{3} \frac{\mathrm{d}}{\mathrm{d}x}\left[\frac{\mathrm{d}\psi}{\mathrm{d}x} \exp\left(3 \int \frac{\bar{h}^2 - 1}{\bar{h}^3} \, \mathrm{d}x\right)\right], \tag{B 9}$$

$$\psi = 0 \qquad \text{at} \qquad x = x_\pm. \tag{B 10}$$

Now, multiply (B 9) by ψ^* (where the asterisk denotes complex conjugate), integrate from x_- to x_+, integrate the right-hand side by parts, and take into account boundary conditions (B 10), which yields

$$\lambda \int_{x_-}^{x_+} \frac{|\psi|^2}{\bar{h}^3} \exp\left(3 \int \frac{\bar{h}^2 - 1}{\bar{h}^3} \, \mathrm{d}x\right) \mathrm{d}x = -\tfrac{1}{3} \int_{x_-}^{x_+} \left|\frac{\mathrm{d}\psi}{\mathrm{d}x}\right|^2 \exp\left(3 \int \frac{\bar{h}^2 - 1}{\bar{h}^3} \, \mathrm{d}x\right) \mathrm{d}x. \tag{B 11}$$

This equality proves that all eigenvalues λ are real and negative–hence, the steady state under consideration is asymptotically stable. Then, in the limit $x_\pm \to \pm\infty$, all λ are real and non-positive, i.e. the steady state is either asymptotically or neutrally stable. (Note that when the region where an eigenvalue problem is defined tends to infinity, some of the eigenvalues may 'accumulate' near zero.)

Observe that, if the boundary conditions were set at infinity from the start, the integrals in (B 11) would have infinite limits and we would need to deal with their convergence (which is not difficult in principle, but involves cumbersome algebra involving large-distance asymptotics of ψ and the coefficients of equation (B 9)).

Appendix C. Conservation of the film's slope at its tip

Denote the film's slope at its tip by s, i.e.

$$s = \left(\frac{\partial h}{\partial x}\right)_{x=-t},$$

and consider

$$\frac{\mathrm{d}s}{\mathrm{d}t} = \left(\frac{\partial^2 h}{\partial t \, \partial x} - \frac{\partial^2 h}{\partial x^2}\right)_{x=-t}. \tag{C 1}$$

Recalling that $h(x, t)$ is governed by the small-slope equation (2.20), one can replace the t-derivative in (C 1) through the x-derivatives and obtain

$$\frac{\mathrm{d}s}{\mathrm{d}t} = \left\{\frac{h^3}{3}\frac{\partial^3 h}{\partial x^3} + h^2\left(\frac{\partial h}{\partial x}\frac{\partial^2 h}{\partial x^2} + \frac{\partial h}{\partial x}\frac{\partial^2 h}{\partial x^2} - \frac{\partial^2 h}{\partial x^2}\right) + 2h\left[\left(\frac{\partial h}{\partial x}\right)^3 - \left(\frac{\partial h}{\partial x}\right)^2\right]\right\}_{x=-t}.$$

Since, by definition, the film's thickness vanishes at the tip (i.e. $(h)_{x=-t} = 0$), the right-hand side of the above equality is zero.

REFERENCES

Bertozzi, A. L. & Brenner, M. P. 1997 Linear stability and transient growth in driven contact lines. *Phys. Fluids* **9**, 530–539.

Derjaguin, B. 1943 Thickness of liquid layer adhering to walls of vessels on their emptying and the theory of photo- and motion-picture film coating. *C. R. (Dokl.) Acad. Sci. URSS* **39**, 13–16.

Derjaguin, B. 1945 On the thickness of the liquid film adhering to the walls of a vessel after emptying. *Acta Physicochim. URSS* **20**, 349–352.

Derjaguin, B. V. & Titievskaya, A. S. 1945 An experimental study of the thickness of a liquid layer left on a rigid wall by a retreating meniscus. *Dokl. Acad. Nauk SSSR* **50**, 30–34.

Dussan V., E. B. 1979 On the spreading of liquids on solid surfaces: static and dynamic contact lines. *Annu. Rev. Fluid Mech.* **11**, 371–400.

Jin, B., Acrivos, A. & Münch, A. 2005 The drag-out problem in film coating. *Phys. Fluids* **17**, 103603.

Kalliadasis, S., Bielarz, C. & Homsy, G. M. 2000 Steady free-surface thin film flows over topography. *Phys. Fluids* **12**, 1889–1898.

Landau, L. & Levich, B. 1942 Dragging of liquid by a plate. *Acta Physiochim. USSR* **17**, 42–54.

Moriarty, J. A., Schwartz, L. W. & Tuck E. O. 1991 Unsteady spreading of thin liquid films with small surface tension. *Phys. Fluids* A **3**, 733–742.

Shikhmurzaev, Y. D. 2006 Singularities at the moving contact line. Mathematical, physical and computational aspects. *Physica* D **217**, 121–133.

Wilson, S. D. R. 1982 The drag-out problem in film coating theory. *J. Engng Maths* **16**, 209–221.